

Dense Text-to-Image Generation with Attention Modulation

Yunji Kim¹

Jiyoung Lee¹

Jin-Hwa Kim¹

Jung-Woo Ha¹

Jun-Yan Zhu²

¹NAVER AI Lab

²Carnegie Mellon University

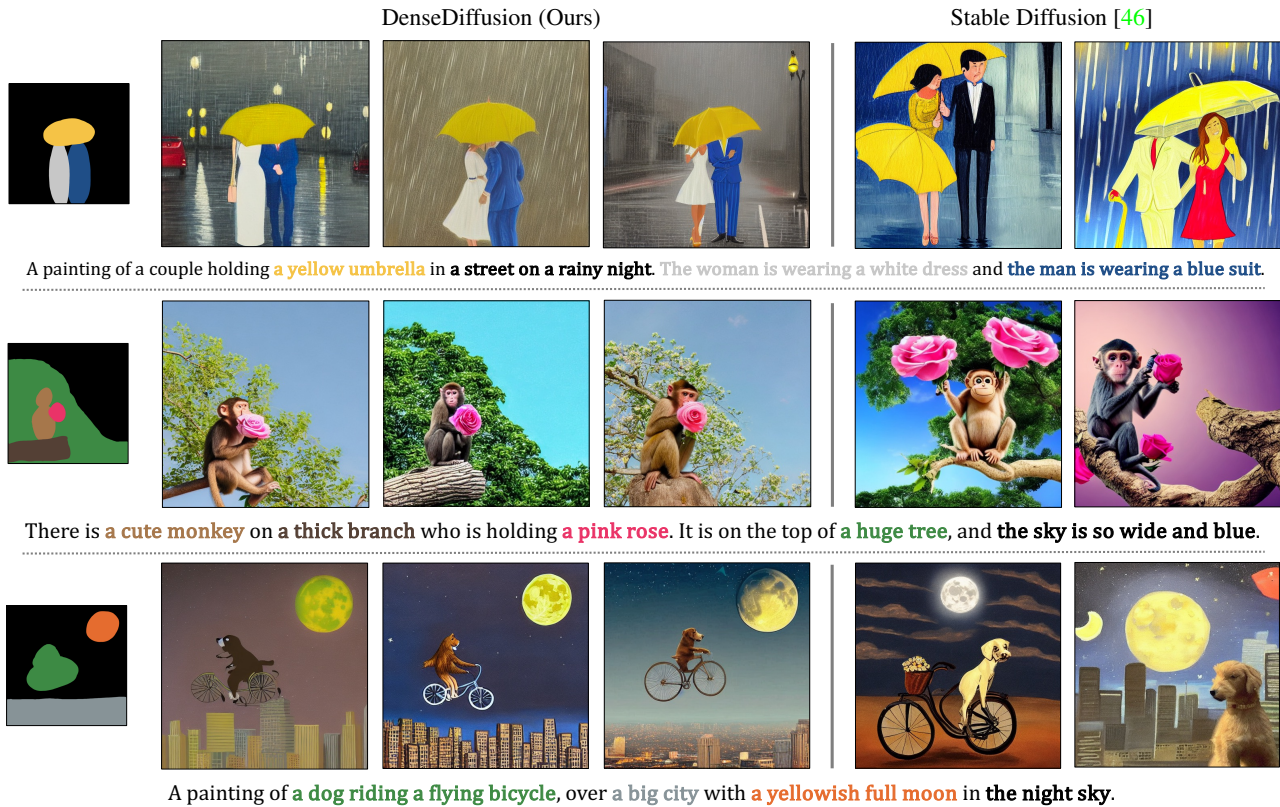


Figure 1: DenseDiffusion enables us to incorporate both text and layout information into pre-trained text-to-image models without requiring additional fine-tuning. Our method not only synthesizes images that follow text prompts more faithfully but also offers users greater control over object and scene layout. We achieve it by modulating attention maps of pre-trained models, such as Stable Diffusion [46], according to both text and layout conditions.

Abstract

Existing text-to-image diffusion models struggle to synthesize realistic images given dense captions, where each text prompt provides a detailed description for a specific image region. To address this, we propose DenseDiffusion, a training-free method that adapts a pre-trained text-to-image model to handle such dense captions while offering control over the scene layout. We first analyze the relationship between generated images' layouts and the pre-trained

model's intermediate attention maps. Next, we develop an attention modulation method that guides objects to appear in specific regions according to layout guidance. Without requiring additional fine-tuning or datasets, we improve image generation performance given dense captions regarding both automatic and human evaluation scores. In addition, we achieve similar-quality visual results with models specifically trained with layout conditions. Code and data are available at <https://github.com/naver-ai/DenseDiffusion>.

1. Introduction

Recently developed text-to-image models can synthesize diverse, high-quality images from short scene descriptions [24, 15, 39, 45, 47, 46, 30, 59, 7]. However, as shown in Figure 1, they often encounter challenges when handling dense captions and tend to omit or blend the visual features of different objects. Here the term “dense” is inspired by the work of dense captioning [28] in which each phrase is used to describe a specific image region. Moreover, it is difficult for users to precisely control the scene layout of a generated image with text prompts alone.

Several recent works propose providing users with spatial control by training or fine-tuning layout-conditioned text-to-image models [2, 55, 60, 34, 46, 19, 57, 38]. While Make-a-Scene [19] and Latent Diffusion Models [46] train models from scratch given both text and layout conditions, other recent and concurrent works, such as SpaText [2] and ControlNet [60], introduce additional spatial controls to existing text-to-image models with model fine-tuning. Unfortunately, training or fine-tuning a model can be computationally-expensive. Moreover, the model needs to be retrained for every new user condition, every new domain, and every new text-to-image base model.

To address the above issue, we propose a training-free method that supports dense captions and offers layout control. We first analyze the intermediate features of a pre-trained text-to-image diffusion model to show that the layout of a generated image is significantly related to self-attention and cross-attention maps. Based on this observation, we modulate intermediate attention maps according to the layout condition on the fly. We further propose considering the value range of original attention scores and adjusting the degree of modulation according to the area of each segment.

Our experiments show that our method improves the performance of Stable Diffusion [46] and outperforms several compositional diffusion models [36, 6, 17] on dense captions regarding both text conditions, layout conditions, and image quality. We verify them using both automatic metrics and user studies. In addition, our method is on par with existing layout-conditioned models regarding qualitative results. Finally, we include a detailed ablation study regarding our design choices and discuss several failure cases. Our code, models, and data are available at <https://github.com/naver-ai/DenseDiffusion>.

2. Related work

Text-to-Image Diffusion Models. The development of large-scale diffusion models [39, 45, 47, 46] has enabled us to synthesize diverse photorealistic images with flexible editing capacity [37, 12, 32, 1, 31]. In particular, recent works [21, 53, 14, 41] edit images by analyzing the interaction between intermediate image features and input

textual features during the generation process. Prompt-to-Prompt [21] extracts cross-attention maps for each text token and injects them when denoising with an edited caption to preserve the input structure. Plug-and-Play [53] takes a similar approach but reuses self-attention and spatial features. pix2pix-zero [41] proposes cross-attention guidance to encourage the cross-attention maps of original and edited images to stay close. Inspired by the above works, we seek to leverage the close connection between the text features and the image layout inside a pre-trained diffusion model but focus on image synthesis with spatial controls rather than image editing.

Compositional Diffusion Methods. Since text-to-image models are typically trained on datasets with short text captions, they often fail to reflect all the details of dense captions composed of several phrases. A line of work tries to address the problem with a pre-trained model in a training-free manner. For example, Composable Diffusion [36] and MultiDiffusion [6] perform a separate denoising process for each phrase at every timestep. Attend-and-Excite [8] optimizes the noise map to increase the activation of the neglected tokens in cross-attention maps. Structure Diffusion [17] indirectly modulates cross-attention scores by enriching textual features for parsed texts.

Meanwhile, similar to the work of Dong et al. [16] that directly increases attention scores of certain words to increase the likelihood of them being generated for language modeling tasks, Paint-with-words (eDiffi-Pww) [4] increases the cross-attention scores between image and text tokens that describe the same object given segmentation masks. However, they sometimes fail to reflect text and layout conditions faithfully. In this work, we propose a more extensive modulation method by devising multiple regularization terms.

Image Synthesis with Spatial Control. Seminal works [11, 29] have proposed data-driven systems for synthesizing images given text descriptions and spatial controls based on image matching and blending. Later, neural networks such as conditional GANs have been adopted to directly synthesize images [27, 10, 58, 40, 52, 61, 26] but only work on limited domains such as natural landscapes or streets. More recently, several works propose to add spatial modulations to a pre-trained text-to-image diffusion model [46, 2, 55, 57, 60, 34]. For example, SpaText [2] fine-tunes a pre-trained model using a paired dataset of images and segmentation maps. ControlNet [60] and GLIGEN [34] develop more effective fine-tuning methods with adapters. Meanwhile, Universal-Guided-Diffusion [5] and Attention Refocusing [42] encourage intermediate outputs to align with the layout condition using guidance functions. Although these models offer control over image layout, they often require retraining each time for a new

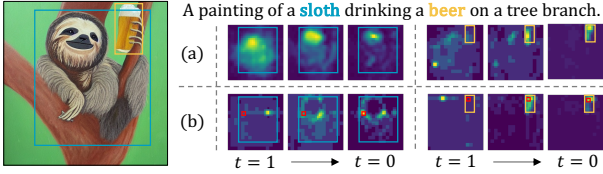


Figure 2: Visualization of 16×16 attention maps attained from (a) cross-attention and (b) self-attention layers of Stable Diffusion [46]. In (a), we visualize the cross-attention maps for “sloth” and “beer”. The objects of interest are outlined with blue and yellow bounding boxes. In (b), we show the attention maps for token keys marked in the red boxes in self-attention layers. As the timestep t approaches zero, tokens affiliated with the same object communicate more closely, influencing the image layout.

type of control or increased inference time.

Several concurrent works also propose training-free spatial control for diffusion models [20, 43, 9]. We encourage the readers to check out their works for more details.

3. Method

Our goal is to improve the text-to-image model’s ability to reflect textual and spatial conditions without fine-tuning. We formally define our condition as a set of N segments $\{(c_n, m_n)\}_{n=1}^N$, where each segment (c_n, m_n) describes a single region, as shown in Figure 3. Here c_n is a non-overlapping part of the full-text caption c , and m_n denotes a binary map representing each region. Given the input conditions, we modulate attention maps of all attention layers on the fly so that the object described by c_n can be generated in the corresponding region m_n . To maintain the pre-trained model’s generation capacity, we design the modulation to consider original value range and each segment’s area.

3.1. Preliminaries

Diffusion Models learn to generate an image by taking successive denoising steps starting from a random noise map z_T [24, 51, 49]. A predefined number of denoising steps determines the degree of noise at each step, and a timestep-dependent noise prediction network ϵ_θ is trained to predict the noise $\tilde{\epsilon}_t$ added to a given input z_t . Although the earlier models, such as DDPM [24], are computationally-expensive, the non-Markovian diffusion method, DDIM [50], has improved the inference speed by drastically reducing the number of denoising steps. More recently, latent diffusion models enable even faster generation with improved image quality [46]. If the task is to generate an image using conditional information c , such as a text caption or semantic segmentation map, the condition can be provided via cross-attention layers. In this work, we experiment with Stable Diffusion [46] and use 50 DDIM denoising steps.

	Matched Key	Unmatched Key
Self-attention Layers (Mean)	0.0148	0.0024
Cross-attention Layers (Mean)	0.0410	0.0122
Cross-attention Layers (Max)	0.0691	0.0372

Table 1: Analysis of attention scores for matched and unmatched keys. First, the object bounding boxes are detected by YOLOv7 [56]. In the context of cross-attention layers, we define a matched key if the key’s text token matches the class label of the box. In self-attention layers, an image token within the box qualifies as a matched key. In both layers, matched keys consistently have higher mean and max attention values than unmatched keys.

Attention Layers. The attention layer [3, 54] is one of the building blocks of Stable Diffusion [46] that updates intermediate features referencing the context features based on the attention maps $A \in \mathbb{R}^{|\text{queries}| \times |\text{keys}|}$ defined as below,

$$A = \text{softmax}\left(\frac{QK^\top}{\sqrt{d}}\right), \quad (1)$$

in which Q and K are query and key values, each mapped from intermediate features and context features. Here d denotes the length of the key and query features.

In a self-attention layer, intermediate features also serve as context features, allowing us to synthesize globally coherent structures by connecting image tokens across different regions. Meanwhile, a cross-attention layer updates conditional on textual features, which are encoded from the input text caption c with a CLIP text encoder [44].

Attention Score Analysis. Previous studies show that text-conditioned diffusion models tend to form the position and appearance of each object in early stages and refine details such as color or texture variations in relatively later stages [13, 4, 18, 21]. We show a similar trend by analyzing 16×16 attention maps produced from Stable Diffusion [46]. We first synthesize images using 250 captions from the MSCOCO validation set [35]. As shown in Figure 2, attention maps tend to resemble the image layout as the generation proceeds. Table 1 shows a quantitative analysis of attention scores, revealing distinct differences based on whether query-key pairs belong to the same object for both cross-attention and self-attention layers. This result suggests that query-key pairs belonging to the same object tend to have larger scores during the generation process.

3.2. Layout-guided Attention Modulation

The analysis results on attention maps motivate us to intervene in the generation process and modulate original scores to better reflect textual and layout conditions. Specifically,

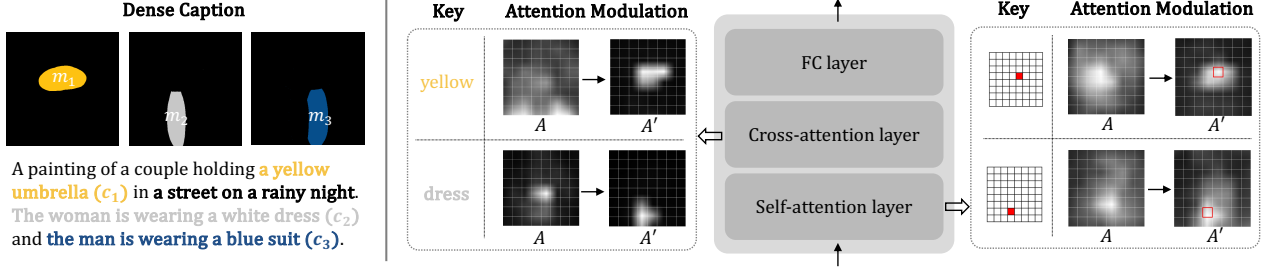


Figure 3: **Our attention modulation process.** Our goal is to congregate specific textual features, denoted as c_n , into the regions defined by its corresponding layout condition m_n . At cross-attention layers, we modulate the attention scores between paired image and text tokens in each segment (c_n, m_n) to have higher values. At self-attention layers, the modulation is applied so that pairs of image tokens belonging to the same object exhibit higher values. In attention maps, brighter colors represent higher attention scores.

we modulate the attention maps as below,

$$\begin{aligned}
 A' &= \text{softmax}\left(\frac{QK^\top + M}{\sqrt{d}}\right), \\
 M &= \lambda_t \cdot R \odot M_{\text{pos}} \odot (1 - S) \\
 &\quad - \lambda_t \cdot (1 - R) \odot M_{\text{neg}} \odot (1 - S),
 \end{aligned} \tag{2}$$

where the query-key pair condition map $R \in \mathbb{R}^{|\text{queries}| \times |\text{keys}|}$ defines whether to increase or decrease the attention score for a particular pair. If two tokens belong to the same segment, they form a positive pair, and their attention score will be increased. If not, they form a negative pair, with their attention decreased.

Due to the difference between cross-attention and self-attention layers, R is defined separately for the two layers. We introduce the matrices $M_{\text{pos}}, M_{\text{neg}} \in \mathbb{R}^{|\text{queries}| \times |\text{keys}|}$ to consider the original value range, which aims to preserve the pre-trained model’s generation capacity. To further adjust the degree of modulation according to the size of each object, we calculate the matrix $S \in \mathbb{R}^{|\text{queries}| \times |\text{keys}|}$ that indicates the segment area for each image query token.

Finally, we observe that a large modification may deteriorate the image quality as the timestep t approaches zero. Therefore, we use a scalar λ_t to adjust the degree of modulation using the power function as below,

$$\lambda_t := w \cdot t^p, \tag{3}$$

where the timestep $t \in [0, 1]$ has been normalized. We use different co-efficients w^c and w^s for cross-attention and self-attention layers.

Attention Modulation at Cross-attention Layers. In cross-attention layers, intermediate image features are updated according to textual features, which construct objects’ appearance and layouts. The degree and location to which they are reflected are determined by the attention scores between image tokens and text tokens. Hence, we modify

cross-attention maps to induce certain textual features congregate in a specific region according to its corresponding layout condition m_n , with the query-key pair condition map R^{cross} defined as below,

$$R_{:j}^{\text{cross}} := \begin{cases} \vec{0}, & \text{if } \vec{k}[j] = 0 \\ \vec{m}_{\vec{k}[j]}, & \text{otherwise} \end{cases}, \tag{4}$$

where \vec{m}_n is a binary map flattened into a vector and resized to match the spatial resolution of each layer. Here $\vec{k} \in \mathbb{R}^{|\text{keys}|}$ is a vector that maps a token index to the segment index. If the j -th text token is not part of any of the N segments, $\vec{k}[j]$ is set to zero.

Attention Modulation at Self-attention Layers. Self-attention layers allow intermediate features to interact with each other to create a globally coherent result. Our attention modulation is designed to restrict communication between tokens of different segments, thereby preventing the mixing of features of distinct objects. Specifically, we increase the attention scores for tokens in the same segment and decrease it for those in different segments. The query-key pair condition map R^{self} for this objective is defined as below,

$$R_{ij}^{\text{self}} := \begin{cases} 1, & \text{if } \exists n \text{ s.t. } \vec{m}_n[i] = 1 \text{ and } \vec{m}_n[j] = 1 \\ 0, & \text{otherwise} \end{cases}. \tag{5}$$

Value-range Adaptive Attention Modulation. Since our method alters the original denoising process, it may potentially compromise the image quality of the pre-trained model. To mitigate this risk, we modulate values according to the range of original attention scores. We calculate the following matrices that identify each query’s maximum and minimum values, ensuring the modulated values stay close to the original range. Therefore, the adjustment is proportional to the difference between the original values and either the maximum value (for positive pairs) or the minimum value (for

negative pairs).

$$\begin{aligned} M_{\text{pos}} &= \max(QK^\top) - QK^\top, \\ M_{\text{neg}} &= QK^\top - \min(QK^\top). \end{aligned} \quad (6)$$

The max and min operations return the maximum and minimum values for each query, initially producing a vector with dimensions $\mathbb{R}^{|\text{queries}| \times 1}$. To restore the original dimensions $\mathbb{R}^{|\text{queries}| \times |\text{keys}|}$, we replicate values along the key-axis.

Mask-area Adaptive Attention Modulation. We observe a noticeable quality degradation when there is a large area difference between segments. Specifically, if one segment’s area is much smaller than others, our method may fail to generate realistic images. To resolve this, we use the matrix S in Equation 2 to automatically adjust the modulation degree according to the area of each segment: increase the degree for small segments and decrease for large segments. To calculate the matrix S , we first compute the area percentage of the mask that each query token belongs to, and then replicate the values along the key axis.

Implementation Details. We use Stable Diffusion [46], trained on the LAION dataset [48]. In our experiments, we only apply the attention modulation to the initial denoising steps ($t = 1 \sim 0.7$), as we observe no clear improvement beyond that. The hyperparameters in Equation 3 are set as follows: $p = 5$, $w^c = 1$ for cross-attention layers, and $w^s = 0.3$ for self-attention layers. To further increase the effectiveness of our method, we replace parts of textual features with separately encoded ones for each text segment c_n . This strategy is particularly useful when a text caption contains multiple closely related objects, such as a microwave and an oven.

4. Experiments

4.1. Evaluation Setting

Baselines. We compare our method with various *training-free* methods, which aim to improve the fidelity of the pre-trained Stable Diffusion [46] when using dense captions. **Composable Diffusion** [36] predicts noises for each phrase separately and merges them at every timestep, leading to a longer inference time proportional to the number of phrases. **Structure Diffusion** [17] employs a language parser to enhance the value features of all parsed phrases at every cross-attention layer. eDiffi-Pww [4] manipulates the attention scores for specific query-key pairs according to an additional layout condition. However, since the eDiffi model is not publicly available, we conduct experiments with the Pww implemented on Stable Diffusion (**SD-Pww**).

	SOA-I \uparrow	CLIP-Score \uparrow	Human Preference \uparrow
Real Images	93.07	0.2821	-
Stable Diffusion [46]	73.08 \pm 1.54	0.2732 \pm 0.0016	62%
Composable Diffusion [36]	55.88 \pm 0.78	0.2507 \pm 0.0023	83%
Structure Diffusion [17]	70.97 \pm 1.08	0.2745 \pm 0.0011	58%
SD-Pww [4]	73.92 \pm 1.84	0.2800 \pm 0.0005	53%
DenseDiffusion (Ours)	77.61 \pm 1.75	0.2814 \pm 0.0005	-

Table 2: Quantitative evaluation results on the fidelity to textual condition. Our method achieves the best performance regarding both automatic metrics and user study. The human preference percentage shows how often AMT participants prefer our results over the baselines.

	IoU \uparrow	Local CLIP-Score \uparrow	Human Preference \uparrow
Real Images	59.13	0.2163	-
SD-Pww [4]	23.76 \pm 0.50	0.2125 \pm 0.0003	63%
DenseDiffusion (Ours)	34.99 \pm 1.13	0.2176 \pm 0.0007	-

Table 3: Quantitative evaluation results on the fidelity to layout condition. We compare only with SD-Pww [4] since it is the only baseline that uses segmentation maps. 63% of AMT participants prefer our results over those from SD-Pww.

Metrics. We evaluate each method regarding two criteria: fidelity to the text prompt and alignment with the layout condition. For text prompt, we calculate the CLIP-Score [22], which measures the distance between input textual features and generated image features, and the SOA-I score [23] that uses YOLOv7 [56] to check if the described objects are present in the generated image. In terms of layout alignment, we compare IoU scores of a segmentation map predicted by YOLOv7 [56], with respect to the given layout condition. We further evaluate CLIP-scores on cropped object images (Local CLIP-score [2]) to check whether generated objects followed detailed descriptions. As Composable Diffusion [36] and Structure Diffusion [17] do not take layout conditions, they are excluded for a fair comparison.

Datasets. We curate a new evaluation dataset containing detailed descriptions for each segment. Specifically, we select 250 samples with two or more unique objects from the MS-COCO validation set [35]. Then we manually replace the class label for each segmentation map with a phrase extracted from the caption; for example, “dog” to “a black and white dog”. We generate four random images per caption, leading to 1,000 images for each baseline used in the evaluation.

User study. We conduct a user study using Amazon Mechanical Turk. For each task, we present users with two sets of 4 images along with the same input conditions. They are

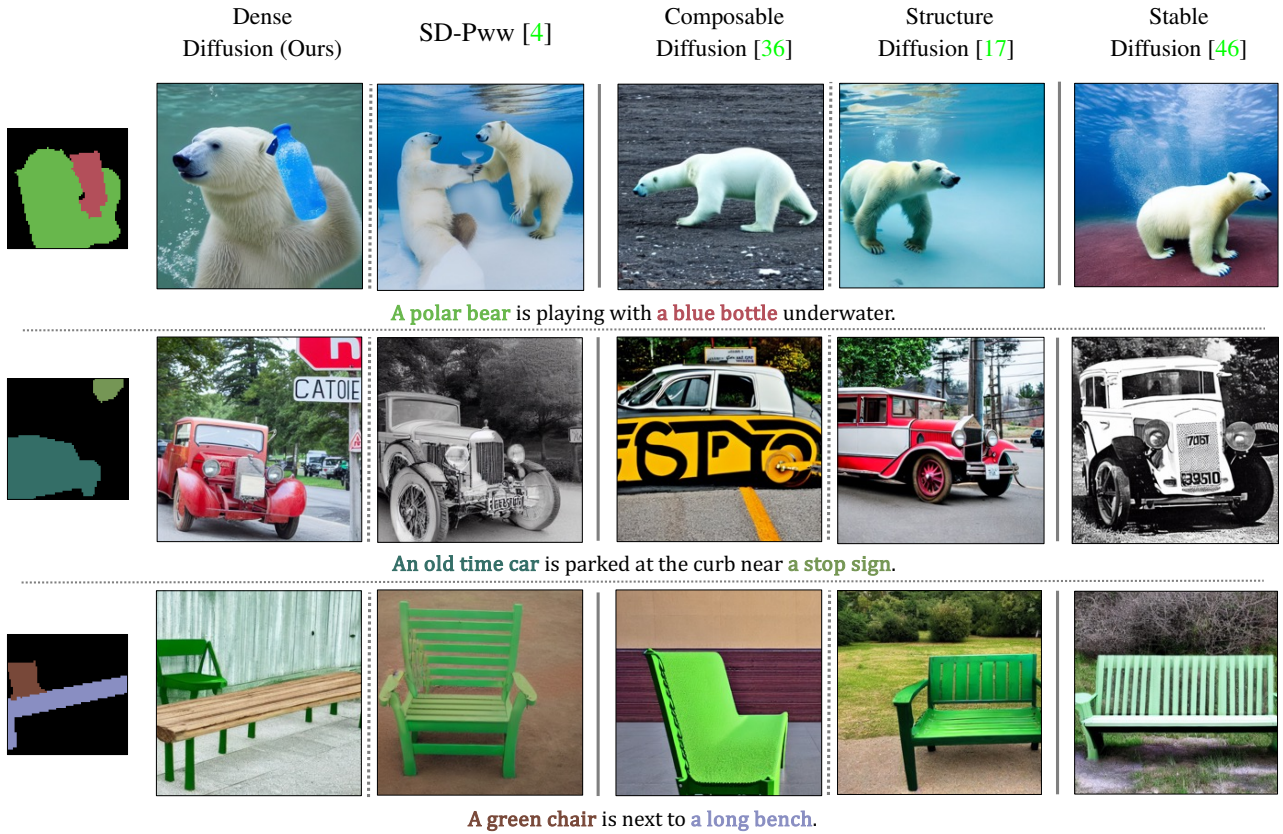


Figure 4: **Comparisons with other training-free methods based on Stable Diffusion [46].** Each image is generated with the same dense caption for all methods. However, only SD-Pww [4] and our method DenseDiffusion support segmentation maps for layout control. Our method aligns more closely with the input mask than SD-Pww [4].

asked to choose the better set based on either of the following criteria: fidelity to the textual condition while reflecting detailed descriptions of key objects or fidelity to the layout condition with accurate depiction of objects. We present each pair in a random order and collect three ratings from unique users. The scores in Table 2 and 3 show the percentage of users who prefer DenseDiffusion over a baseline. 50% means that DenseDiffusion and a baseline have the same preference, and values more than 50% indicate that more users select DenseDiffusion instead of the baseline.

4.2. Results

Evaluation on the fidelity to textual condition. In Figure 4, we compare DenseDiffusion with all baselines for images generated with dense captions. While baseline methods sometimes omit one or more objects described in the text captions, our results are more faithful to both textual and layout conditions. In particular, the comparison with SD-Pww [4] highlights the effectiveness of our training-free modulation method.

The quantitative evaluation results in Table 2 reveal a consistent trend. DenseDiffusion outperforms others in terms

of both automatic and human evaluation. However, SOA-I seems to be loosely correlated with the human evaluation results due to the domain gap between LAION [48] and MS-COCO [35], used for training Stable Diffusion [46] and YOLOv7 [56] respectively. Interestingly, the performance tends to suffer significantly when the inference method is altered too much from the original one, as seen in the case of Composable Diffusion [36].

Evaluation on the fidelity to layout condition. To evaluate the fidelity to layout conditions, we only compare with the results of SD-Pww [4], the only baseline that can control an image layout. Figures 4, 5 and Table 3 show that DenseDiffusion outperforms SD-Pww by a large margin. SD-Pww not only fails to reflect layout conditions faithfully but also tends to mix different object features or omits key objects. In particular, the substantial difference in IoU scores shows that DenseDiffusion is more effective in reflecting layout conditions. Figure 6 shows that our method responds well to various conditions created by changing part of a given textual condition, such as object types or image styles while maintaining the original layout condition.

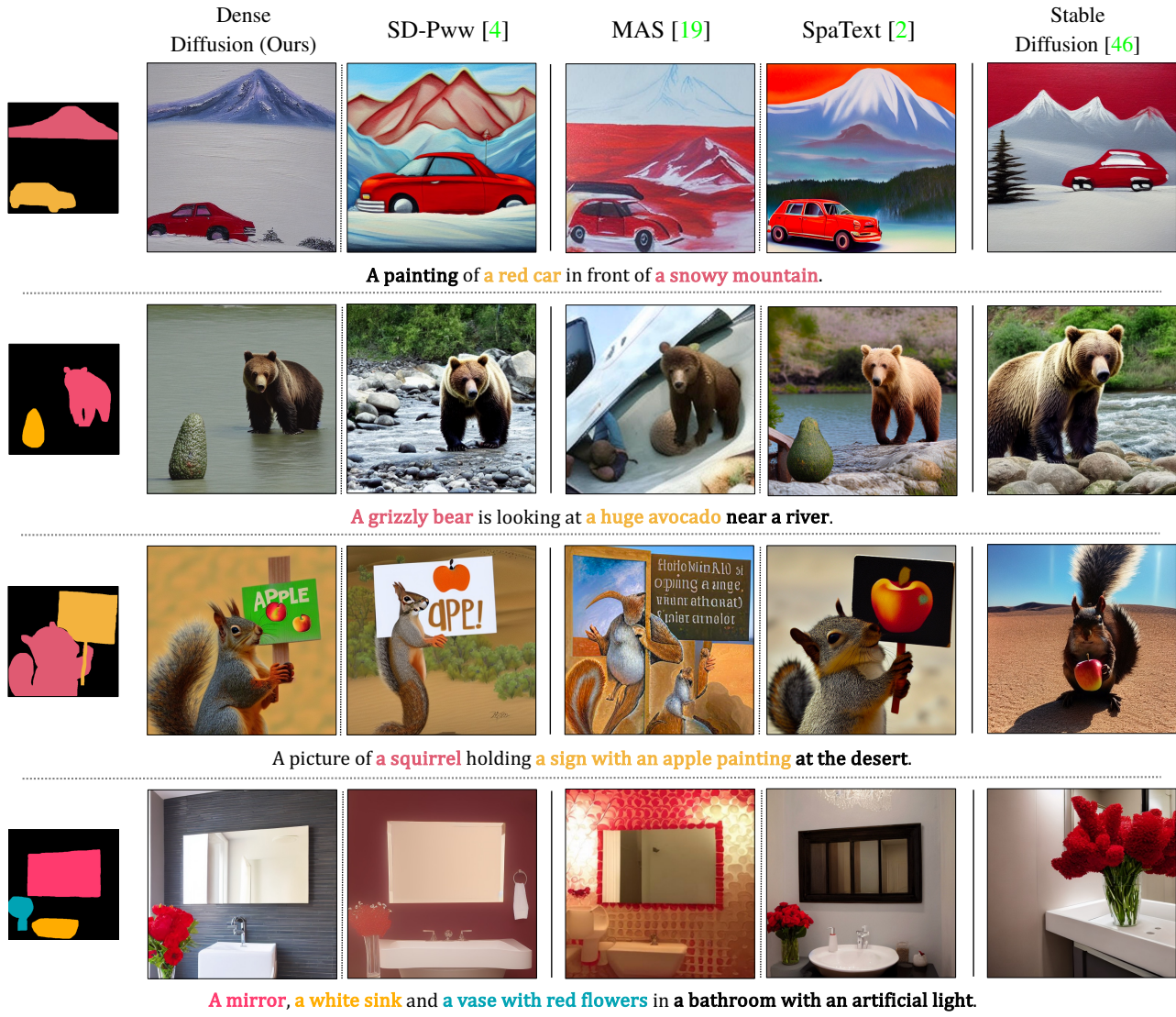


Figure 5: Comparison with different layout-guided text-to-image methods. While MAS [19] and SpaText [2] are specifically trained for layout control, SD-Pww [4] and DenseDiffusion (ours) are training-free methods based on pre-trained Stable Diffusion models [46]. Nevertheless, our results adhere to layout conditions comparably to SpaText [2], and even outperform MAS [19] in many cases.

Comparison to layout-conditioned models. To highlight that DenseDiffusion is effective even as a training-free method, we further compare with MAS [19] and SpaText [2], both of which are text-to-image models trained with layout conditions. MAS [19] uses tokenized semantic segmentation maps as an additional condition, and SpaText [2] fine-tunes Stable Diffusion [46] with spatially splatted CLIP image features according to a layout condition. Since these models are not publicly available, we use the examples presented in the original SpaText paper. Figure 5 shows that DenseDiffusion can reflect layout conditions comparably and even outperforms MAS [19] for diverse concepts. Please refer to Appendix A for more additional comparisons and results.

Ablation Study. Below we evaluate each component used in our DenseDiffusion: (a) Attention Modulation at Cross-attention Layers, (b) Attention Modulation at Self-attention Layers, (c) Value-range Adaptive Attention Modulation, and (d) Mask-area Adaptive Attention Modulation.

We first present visual results from our ablation study in Figure 7. All images in the same row are generated from the same initial noise map. As shown in columns w/o (a) and w/o (b), attention modulations in both cross-attention and self-attention layers are crucial for satisfying both textual and layout conditions. The images in column w/o (c) show that value-range adaptive modulation improves the fidelity of the method to given conditions further. Finally, according

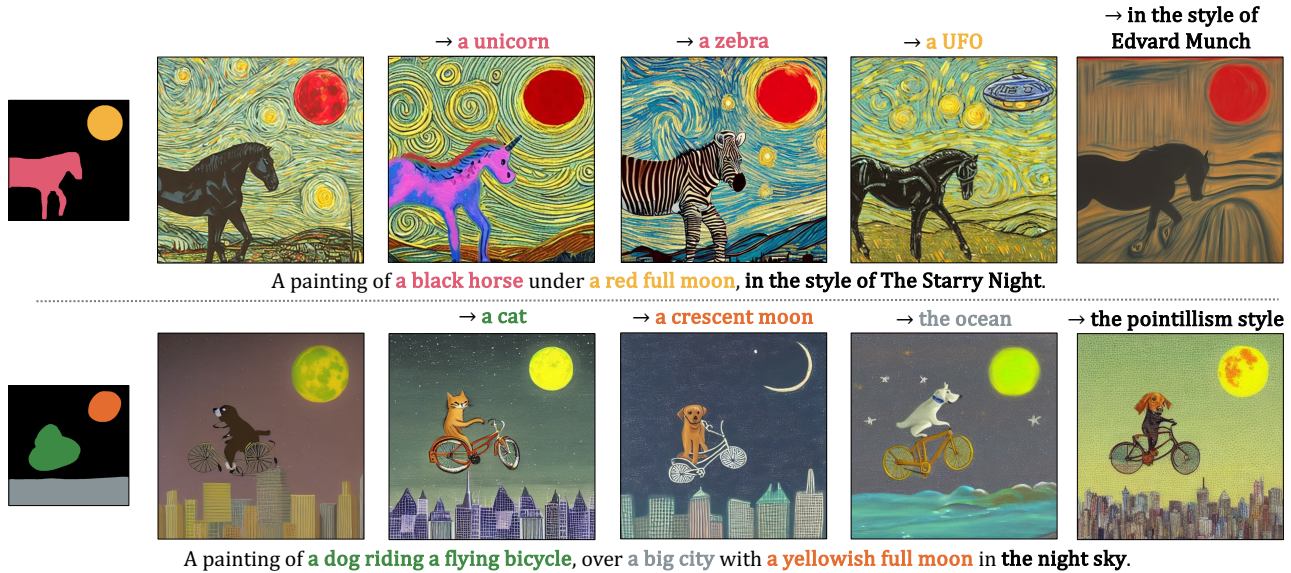


Figure 6: We generate images using the same layout condition but with various text prompts, by modifying part of the given textual condition. Our results faithfully adhere to both textual and layout conditions.



Figure 7: **Ablation study.** We show some example results when various components are ablated from our full method. We define the following components as: (a) Attention Modulation at Cross-attention Layers, (b) Attention Modulation at Self-attention Layers, (c) Value-range Adaptive Attention Modulation, and (d) Mask-area Adaptive Attention Modulation. All images are generated with the same initial noise map. We can infer that all components contribute to improving the fidelity of Stable Diffusion to the given conditions.

to column **w/o (d)**, the method adheres to the conditions but produces images with monotonous textures.

In Table 4, we evaluate various ablated methods using automatic metrics. The results show that, except for component (d), the removal of each component leads to a significant drop in all metric scores. As indicated by the significant drops in IoU scores, the ablated methods fail to achieve high fidelity to layout conditions. The largest performance degradation is observed when attention modulation at cross-

attention layers is omitted, as textual features play a crucial role in constructing the image layout. Furthermore, modulating scores without considering the value-range also results in drops across all metrics. These findings collectively confirm that our attention modulation is highly effective in improving the fidelity to given conditions without compromising the generation capability of the pre-trained model.

Regarding component (d), we interpret this exception as a result of the ablated method’s tendency to create a

	SOA-I \uparrow	CLIP-Score \uparrow	IoU \uparrow	Local CLIP-Score \uparrow
w/o (a)	72.27	0.2785	18.35	0.2050
w/o (b)	75.60	0.2790	29.57	0.2152
w/o (c)	76.51	0.2801	29.88	0.2136
w/o (d)	73.62	0.2808	38.00	0.2191
DenseDiffusion	77.61	0.2814	34.99	0.2176

Table 4: **Quantitative evaluations on each component.** We evaluate several variants, in which the following components are removed from our full method: (a) Attention Modulation at Cross-attention Layers, (b) Attention Modulation at Self-attention Layers, (c) Value-range Adaptive Attention Modulation, and (d) Mask-area Adaptive Attention Modulation. The results suggest that each component contributes to the final performance of DenseDiffusion.

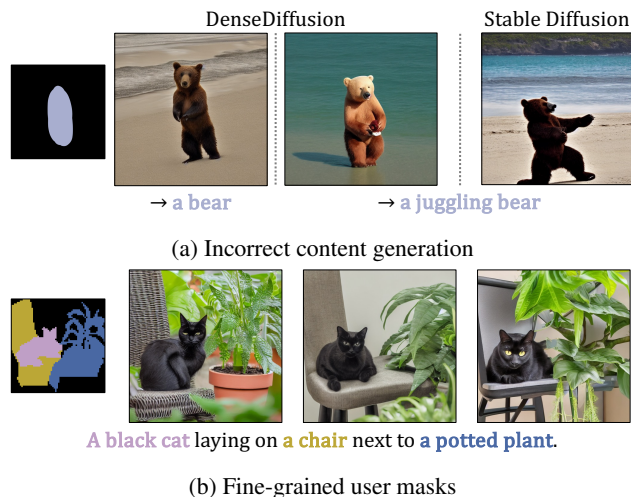


Figure 8: **Limitations and failure cases.** (a) Given captions, “a photo of (a bear / a juggling bear) at the beach”, our method fails in the latter case, since the Stable Diffusion itself cannot generate an image with the correct appearance. (b) As both self-attention and cross-attention layers are fairly coarse, our method fails to follow fine details of the segment condition, such as the shape of leaves.

monotonous background, as shown in Figure 7. While it may seem distant from a realistic image, it is easier for the segmentation model to predict a segmentation map. Hence, it helps to get good scores on metrics related to layout conditions, but it does not always satisfy the textual conditions.

5. Conclusion

In this work, we have proposed DenseDiffusion, a training-free method that improves the fidelity of a pre-trained text-to-image model to dense captions, and enable image layout control. Our finding shows that considering the value range and segment size significantly improves our attention modulation method. Experimental results show that DenseDiffusion outperform other methods on various evaluation metrics. Notably, our training-free method pro-

vides comparable layout control to existing models that are specifically trained for this task.

Limitations. DenseDiffusion has several limitations. First, our method is highly dependent on the capacity of its base model, Stable Diffusion [46]. As shown in Figure 8a, our method fails to produce certain objects, such as a juggling bear, if Stable Diffusion is unable to produce them itself.

Second, our method struggles with fine-grained input masks with thin structures, as both self-attention and cross-attention layers are fairly coarse. As examples shown in Figure 8b, our method fails to follow fine details of the segment condition, such as the shape of leaves.

Acknowledgments. We thank Or Patashnik and Songwei Ge for paper proofreading and helpful comments. This work was experimented on the NAVER Smart Machine Learning (NSML) platform [33].

References

- [1] Omri Avrahami, Ohad Fried, and Dani Lischinski. Blended latent diffusion. In *arXiv preprint arXiv:2206.02779*, 2022. 2
- [2] Omri Avrahami, Thomas Hayes, Oran Gafni, Sonal Gupta, Yaniv Taigman, Devi Parikh, Dani Lischinski, Ohad Fried, and Xi Yin. Spatext: Spatio-textual representation for controllable image generation. In *CVPR*, 2023. 2, 5, 7
- [3] Dzmitry Bahdanau, Kyunghyun Cho, and Yoshua Bengio. Neural machine translation by jointly learning to align and translate. *arXiv preprint arXiv:1409.0473*, 2014. 3
- [4] Yogesh Balaji, Seungjun Nah, Xun Huang, Arash Vahdat, Jiaming Song, Karsten Kreis, Miika Aittala, Timo Aila, Samuli Laine, Bryan Catanzaro, Tero Karras, and Ming-Yu Liu. ediff-i: Text-to-image diffusion models with ensemble of expert denoisers. In *arXiv*, 2022. 2, 3, 5, 6, 7, 12
- [5] Arpit Bansal, Hong-Min Chu, Avi Schwarzschild, Soumyadip Sengupta, Micah Goldblum, Jonas Geiping, and Tom Goldstein. Universal guidance for diffusion models. In *arXiv*, 2023. 2, 12
- [6] Omer Bar-Tal, Lior Yariv, Yaron Lipman, and Tali Dekel. Multidiffusion: Fusing diffusion paths for controlled image generation. In *ICML*, 2023. 2, 12
- [7] Huiwen Chang, Han Zhang, Jarred Barber, AJ Maschinot, Jose Lezama, Lu Jiang, Ming-Hsuan Yang, Kevin Murphy, William T Freeman, Michael Rubinstein, et al. Muse: Text-to-image generation via masked generative transformers. In *ICML*, 2023. 2
- [8] Hila Chefer, Yuval Alaluf, Yael Vinker, Lior Wolf, and Daniel Cohen-Or. Attend-and-excite: Attention-based semantic guidance for text-to-image diffusion models. In *SIGGRAPH*, 2023. 2, 12
- [9] Minghao Chen, Iro Laina, and Andrea Vedaldi. Training-free layout control with cross-attention guidance. *arXiv preprint arXiv:2304.03373*, 2023. 3

- [10] Qifeng Chen and Vladlen Koltun. Photographic image synthesis with cascaded refinement networks. In *ICCV*, 2017. [2](#)
- [11] Tao Chen, Ming-Ming Cheng, Ping Tan, Ariel Shamir, and Shi-Min Hu. Sketch2photo: Internet image montage. *ACM transactions on graphics (TOG)*, 28(5):1–10, 2009. [2](#)
- [12] Jooyoung Choi, Sungwon Kim, Yonghyun Jeong, Youngjune Gwon, and Sungroh Yoon. Ilvr: Conditioning method for denoising diffusion probabilistic models. In *ICCV*, 2021. [2](#)
- [13] Jooyoung Choi, Jungbeom Lee, Chaehun Shin, Sungwon Kim, Hyunwoo Kim, and Sungroh Yoon. Perception prioritized training of diffusion models. In *CVPR*, 2022. [3](#)
- [14] Guillaume Couairon, Jakob Verbeek, Holger Schwenk, and Matthieu Cord. Diffedit: Diffusion-based semantic image editing with mask guidance. In *ICLR*, 2023. [2](#)
- [15] Prafulla Dhariwal and Alexander Nichol. Diffusion models beat gans on image synthesis. 2021. [2](#)
- [16] Yue Dong, Chandra Bhagavatula, Ximing Lu, Jena D. Hwang, Antoine Bosselut, Jackie Chi Kit Cheung, and Yejin Choi. On-the-fly attention modulation for neural generation. In *ACL*, 2021. [2](#)
- [17] Weixi Feng, Xuehai He, Tsu-Jui Fu, Varun Jampani, Arjun Akula, Pradyumna Narayana, Sugato Basu, Xin Eric Wang, and William Yang Wang. Training-free structured diffusion guidance for compositional text-to-image synthesis. In *ICLR*, 2023. [2](#), [5](#), [6](#), [12](#)
- [18] Zhida Feng, Zhenyu Zhang, Xintong Yu, Yewei Fang, Lanxin Li, Xuyi Chen, Yuxiang Lu, Jiayang Liu, Weichong Yin, Shikun Feng, Yu Sun, Hao Tian, Hua Wu, and Haifeng Wang. Ernie-vilg 2.0: Improving text-to-image diffusion model with knowledge-enhanced mixture-of-denoising-experts. In *arXiv*, 2022. [3](#)
- [19] Oran Gafni, Adam Polyak, Oron Ashual, Shelly Sheynin, Devi Parikh, and Yaniv Taigman. Make-a-scene: Scene-based text-to-image generation with human priors. In *ECCV*, 2022. [2](#), [7](#)
- [20] Yutong He, Ruslan Salakhutdinov, and J Zico Kolter. Localized text-to-image generation for free via cross attention control. *arXiv preprint arXiv:2306.14636*, 2023. [3](#)
- [21] Amir Hertz, Ron Mokady, Jay Tenenbaum, Kfir Aberman, Yael Pritch, and Daniel Cohen-Or. Prompt-to-prompt image editing with cross attention control. In *arXiv*, 2022. [2](#), [3](#)
- [22] Jack Hessel, Ari Holtzman, Maxwell Forbes, Ronan Le Bras, and Yejin Choi. Clipscore: A reference-free evaluation metric for image captioning. In *EMNLP*, 2021. [5](#)
- [23] Tobias Hinz, Stefan Heinrich, and Stefan Wermter. Semantic object accuracy for generative text-to-image synthesis. In *TPAMI*, 2020. [5](#)
- [24] Jonathan Ho, Ajay Jain, and Pieter Abbeel. Denoising diffusion probabilistic models. In *NeurIPS*, 2020. [2](#), [3](#)
- [25] Andrew Howard, Mark Sandler, Grace Chu, Liang-Chieh Chen, Bo Chen, Mingxing Tan, Weijun Wang, Yukun Zhu, Ruoming Pang, Vijay Vasudevan, Quoc V. Le, and Hartwig Adam. Searching for mobilenetv3. In *ICCV*, 2019. [12](#)
- [26] Xun Huang, Arun Mallya, Ting-Chun Wang, and Ming-Yu Liu. Multimodal conditional image synthesis with product-of-experts gans. In *ECCV*. Springer, 2022. [2](#)
- [27] Phillip Isola, Jun-Yan Zhu, Tinghui Zhou, and Alexei A Efros. Image-to-image translation with conditional adversarial networks. In *CVPR*, 2017. [2](#)
- [28] Justin Johnson, Andrej Karpathy, and Li Fei-Fei. Denscap: Fully convolutional localization networks for dense captioning. In *CVPR*, 2016. [2](#)
- [29] Matthew Johnson, Gabriel J Brostow, Jamie Shotton, Ognjen Arandjelovic, Vivek Kwatra, and Roberto Cipolla. Semantic photo synthesis. In *Computer graphics forum*, volume 25, pages 407–413. Wiley Online Library, 2006. [2](#)
- [30] Minguk Kang, Jun-Yan Zhu, Richard Zhang, Jaesik Park, Eli Shechtman, Sylvain Paris, and Taesung Park. Scaling up gans for text-to-image synthesis. In *CVPR*, 2023. [2](#)
- [31] Bahjat Kawar, Shiran Zada, Oran Lang, Omer Tov, Huiwen Chang, Tali Dekel, Inbar Mosseri, and Michal Irani. Imagic: Text-based real image editing with diffusion models. In *CVPR*, 2023. [2](#)
- [32] Gwanghyun Kim, Taesung Kwon, and Jong Chul Ye. Diffusionclip: Text-guided diffusion models for robust image manipulation. In *CVPR*, 2022. [2](#)
- [33] Hanjoo Kim, Minkyu Kim, Dongjoo Seo, Jinwoong Kim, Heungseok Park, Soeun Park, Hyunwoo Jo, KyungHyun Kim, Youngil Yang, Youngkwan Kim, et al. Nsml: Meet the mlaas platform with a real-world case study. In *arXiv*, 2018. [9](#)
- [34] Yuheng Li, Haotian Liu, Qingyang Wu, Fangzhou Mu, Jianwei Yang, Jianfeng Gao, Chunyuan Li, and Yong Jae Lee. Gligen: Open-set grounded text-to-image generation. In *arXiv*, 2023. [2](#)
- [35] Tsung-Yi Lin, Michael Maire, Serge Belongie, Lubomir Bourdev, Ross Girshick, James Hays, Pietro Perona, Deva Ramanan, C. Lawrence Zitnick, and Piotr Dollár. Microsoft coco: Common objects in context. In *ECCV*, 2014. [3](#), [5](#), [6](#), [12](#)
- [36] Nan Liu, Shuang Li, Yilun Du, Antonio Torralba, and Joshua B Tenenbaum. Compositional visual generation with composable diffusion models. In *ECCV*, 2022. [2](#), [5](#), [6](#), [12](#)
- [37] Chenlin Meng, Yang Song, Jiaming Song, Jiajun Wu, Jun-Yan Zhu, and Stefano Ermon. Sdedit: Image synthesis and editing with stochastic differential equations. In *ICLR*, 2021. [2](#)
- [38] Chong Mou, Xintao Wang, Liangbin Xie, Jian Zhang, Zhonggang Qi, Ying Shan, and Xiaohu Qie. T2i-adapter: Learning adapters to dig out more controllable ability for text-to-image diffusion models. *arXiv preprint arXiv:2302.08453*, 2023. [2](#)
- [39] Alex Nichol, Prafulla Dhariwal, Aditya Ramesh, Pranav Shyam, Pamela Mishkin, Bob McGrew, Ilya Sutskever, and Mark Chen. Glide: Towards photorealistic image generation and editing with text-guided diffusion models. In *ICML*, 2022. [2](#)
- [40] Taesung Park, Ming-Yu Liu, Ting-Chun Wang, and Jun-Yan Zhu. Semantic image synthesis with spatially-adaptive normalization. In *CVPR*, 2019. [2](#)
- [41] Gaurav Parmar, Krishna Kumar Singh, Richard Zhang, Yijun Li, Jingwan Lu, and Jun-Yan Zhu. Zero-shot image-to-image translation. In *SIGGRAPH*, 2023. [2](#)
- [42] Quynh Phung, Songwei Ge, and Jia-Bin Huang. Grounded text-to-image synthesis with attention refocusing. In *arXiv*, 2023. [2](#)

- [43] Quynh Phung, Songwei Ge, and Jia-Bin Huang. Grounded text-to-image synthesis with attention refocusing. *arXiv preprint arXiv:2306.05427*, 2023. 3
- [44] Alec Radford, Jong Wook Kim, Chris Hallacy, Aditya Ramesh, Gabriel Goh, Sandhini Agarwal, Girish Sastry, Amanda Askell, Pamela Mishkin, Jack Clark, Gretchen Krueger, and Ilya Sutskever. Learning transferable visual models from natural language supervision. In *ICML*, 2021. 3
- [45] Aditya Ramesh, Prafulla Dhariwal, Alex Nichol, Casey Chu, and Mark Chen. Hierarchical text-conditional image generation with clip latents. In *arXiv*, 2022. 2
- [46] Robin Rombach, Andreas Blattmann, Dominik Lorenz, Patrick Esser, and Björn Ommer. High-resolution image synthesis with latent diffusion models. In *CVPR*, 2022. 1, 2, 3, 5, 6, 7, 9, 12
- [47] Chitwan Saharia, William Chan, Saurabh Saxena, Lala Li, Jay Whang, Emily Denton, Seyed Kamyar Seyed Ghasemipour, Burcu Karagol Ayan, S Sara Mahdavi, Rapha Gontijo Lopes, et al. Photorealistic text-to-image diffusion models with deep language understanding. In *NeurIPS*, 2022. 2
- [48] Christoph Schuhmann, Romain Beaumont, Richard Vencu, Cade Gordon, Ross Wightman, Mehdi Cherti, Theo Coombes, Aarush Katta, Clayton Mullis, Mitchell Wortsman, Patrick Schramowski, Srivatsa Kundurthy, Katherine Crowson, Ludwig Schmidt, Robert Kaczmarczyk, and Jenia Jitsev. Laion-5b: An open large-scale dataset for training next generation image-text models. In *NeurIPS Track on Datasets and Benchmarks*, 2022. 5, 6
- [49] Jascha Sohl-Dickstein, Eric Weiss, Niru Maheswaranathan, and Surya Ganguli. Deep unsupervised learning using nonequilibrium thermodynamics. In *ICML*, 2015. 3
- [50] Jiaming Song, Chenlin Meng, and Stefano Ermon. Denoising diffusion implicit models. In *ICLR*, 2020. 3
- [51] Yang Song, Jascha Sohl-Dickstein, Diederik P Kingma, Abhishek Kumar, Stefano Ermon, and Ben Poole. Score-based generative modeling through stochastic differential equations. In *ICLR*, 2021. 3
- [52] Vadim Sushko, Edgar Schönfeld, Dan Zhang, Juergen Gall, Bernt Schiele, and Anna Khoreva. You only need adversarial supervision for semantic image synthesis. *arXiv preprint arXiv:2012.04781*, 2020. 2
- [53] Narek Tumanyan, Michal Geyer, Shai Bagon, and Tali Dekel. Plug-and-play diffusion features for text-driven image-to-image translation. In *arXiv*, 2022. 2
- [54] Ashish Vaswani, Noam Shazeer, Niki Parmar, Jakob Uszkoreit, Llion Jones, Aidan N Gomez, Łukasz Kaiser, and Illia Polosukhin. Attention is all you need. In *NeurIPS*, 2017. 3
- [55] Andrey Voynov, Kfir Abernan, and Daniel Cohen-Or. Sketch-guided text-to-image diffusion models. In *arXiv*, 2022. 2
- [56] Chien-Yao Wang, Alexey Bochkovskiy, and Hong-Yuan Mark Liao. YOLOv7: Trainable bag-of-freebies sets new state-of-the-art for real-time object detectors. In *arXiv*, 2022. 3, 5, 6
- [57] Tengfei Wang, Ting Zhang, Bo Zhang, Hao Ouyang, Dong Chen, Qifeng Chen, and Fang Wen. Pretraining is all you need for image-to-image translation. *arXiv preprint arXiv:2205.12952*, 2022. 2
- [58] Ting-Chun Wang, Ming-Yu Liu, Jun-Yan Zhu, Andrew Tao, Jan Kautz, and Bryan Catanzaro. High-resolution image synthesis and semantic manipulation with conditional gans. In *CVPR*, 2018. 2
- [59] Jiahui Yu, Yuanzhong Xu, Jing Yu Koh, Thang Luong, Gungjan Baid, Zirui Wang, Vijay Vasudevan, Alexander Ku, Yinfei Yang, Burcu Karagol Ayan, et al. Scaling autoregressive models for content-rich text-to-image generation. *arXiv preprint arXiv:2206.10789*, 2(3):5, 2022. 2
- [60] Lvmin Zhang and Maneesh Agrawala. Adding conditional control to text-to-image diffusion models. In *arXiv*, 2023. 2
- [61] Peihao Zhu, Rameen Abdal, Yipeng Qin, and Peter Wonka. Sean: Image synthesis with semantic region-adaptive normalization. In *CVPR*, 2020. 2

A. Additional Comparison

Here, we present additional qualitative results generated by concurrent works on several dense captions. Specifically, three captions are selected from MS-COCO [35], and the other three are curated by the authors.

A.1. Baselines

We compare to the following baselines, which also address the limitations of pre-trained text-to-image diffusion models, including (1) object omission or the mixing of visual features from different objects and (2) the lack of spatial controls. All the methods are implemented on or fine-tuned using the Stable Diffusion [46].

Both **Attend-and-Excite** [8] and **Universal-Guided-Diffusion** [5] modify the inference algorithm with additional objectives. Attend-and-Excite [8] encourages the subject text tokens to be active in cross-attention layers. This method does not support additional layout conditions. Universal-Guided-Diffusion [5] utilizes off-the-shelf segmentation network, MobileNetV3 [25], to incorporate additional guidance. Specifically, it induces the mask inferred from the predicted clean image to match the given conditional mask. However, since MobileNetV3 is trained on MS-COCO dataset, they cannot be applied to our curated prompts that contain out-of-domain objects. We only report their results on our MS-COCO prompts. Meanwhile, **MultiDiffusion** [6] adopts an independent denoising process for each phrase, and use the layout masks to blend the predicted noises. These three training-free methods are much slower than the original inference method, as their inference time is proportional to the number of objects.

A.2. Results

Figures 9, 10, and 11 show results for our curated prompts, and Figures 12, 13, and 14 show results for MS-COCO prompts. We observe that our attention modulation method is more effective than SD-Pww [4] and Structure Diffusion [17] regarding the fidelity to textual and layout conditions.

MultiDiffusion [6] accurately reflects objects, but the results often look like collages of multiple objects, due to the lack of interaction between independent denoising processes. Meanwhile, Composable Diffusion [36], Attend-and-Excite [8] and Universal-Guided-Diffusion [5] often fail to follow the conditions well and tend to generate unrealistic images.

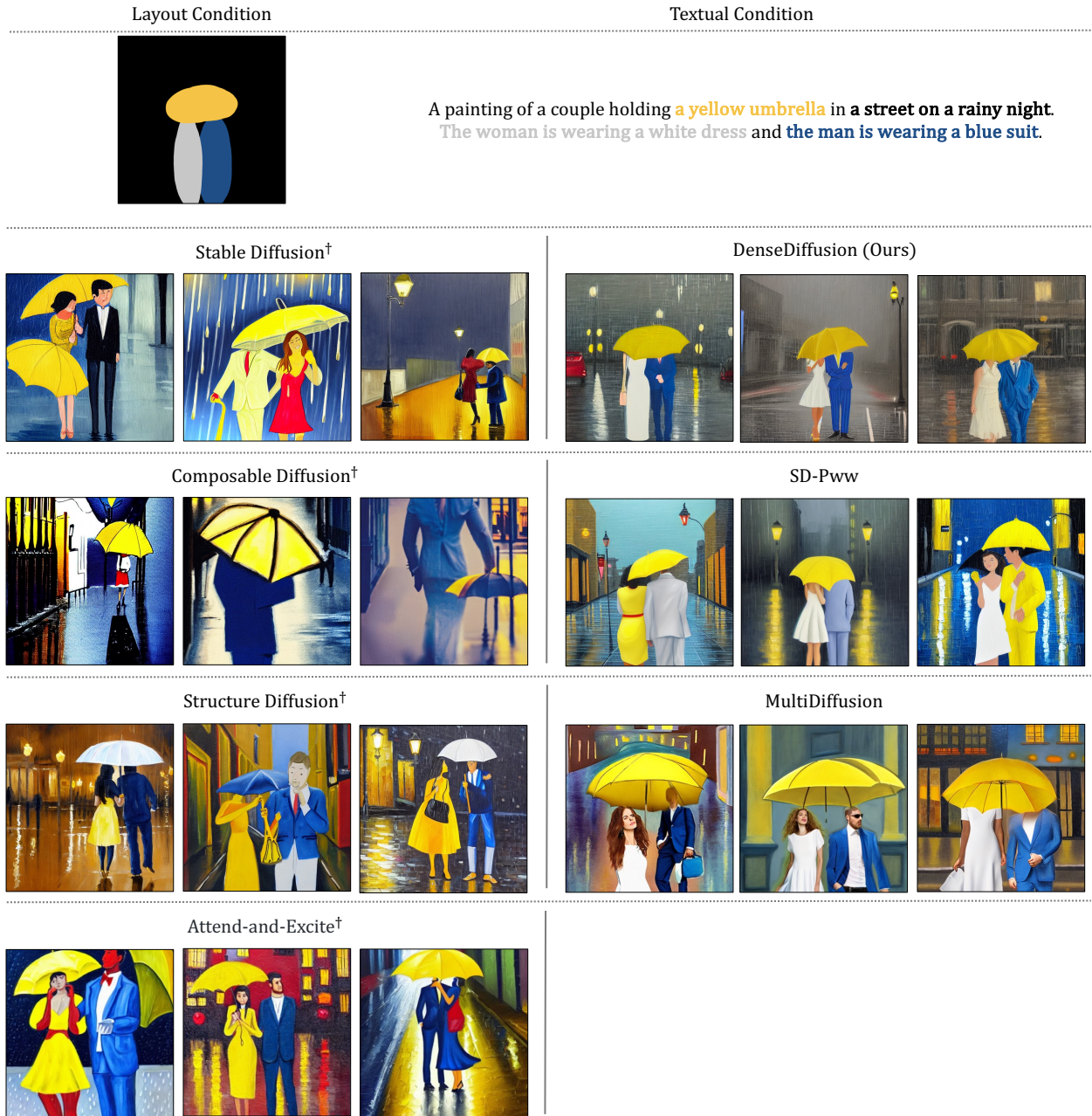


Figure 9: Qualitative comparison with additional methods. Methods denoted with [†] receive textual condition only.

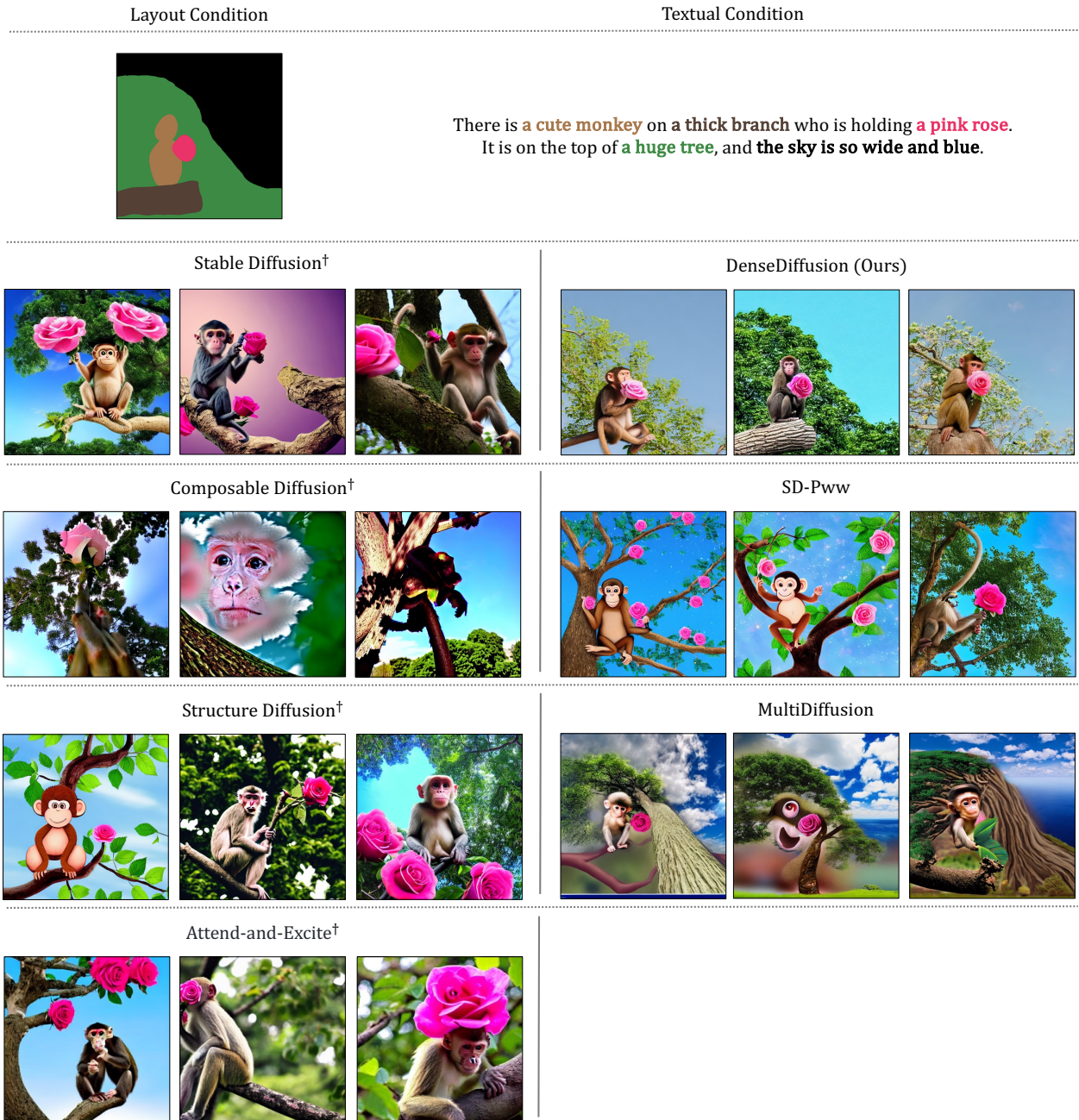


Figure 10: Qualitative comparison with additional methods. Methods denoted with [†] receive textual condition only.

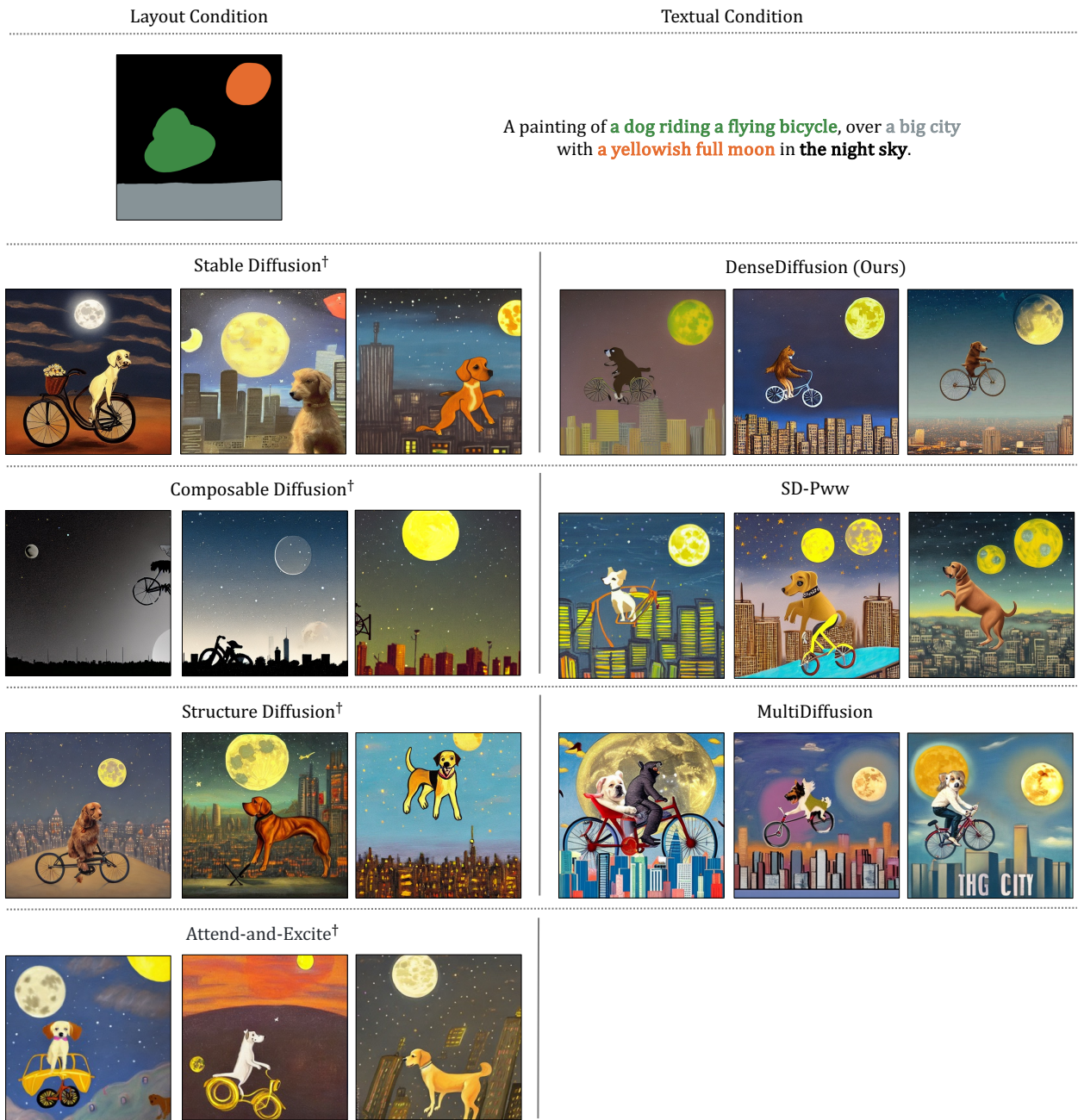


Figure 11: Qualitative comparison with additional methods. Methods denoted with [†] receive textual condition only.

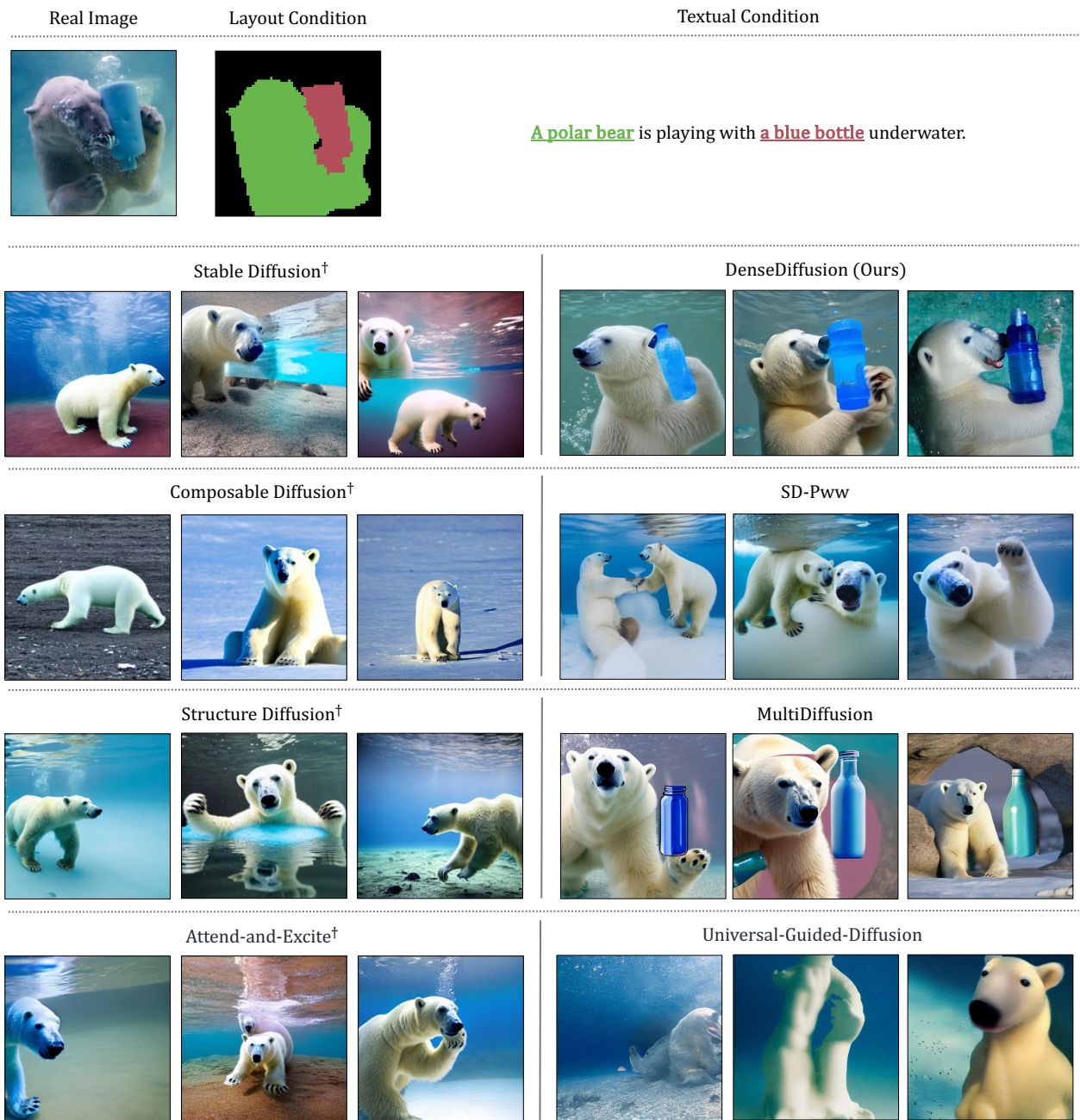


Figure 12: Qualitative comparison with additional methods. Methods denoted with [†] receive textual condition only.

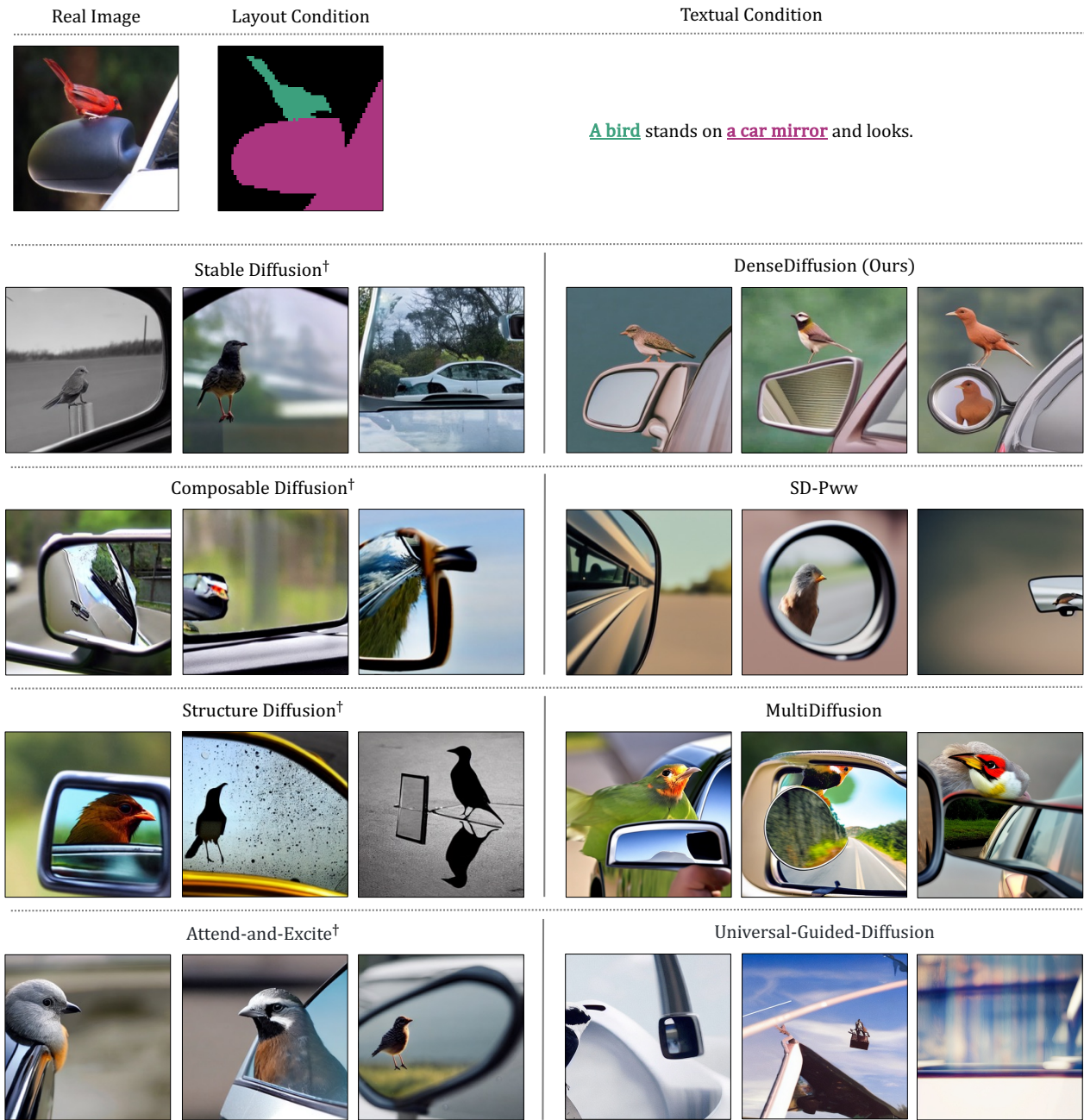


Figure 13: Qualitative comparison with additional methods. Methods denoted with [†] receive textual condition only.

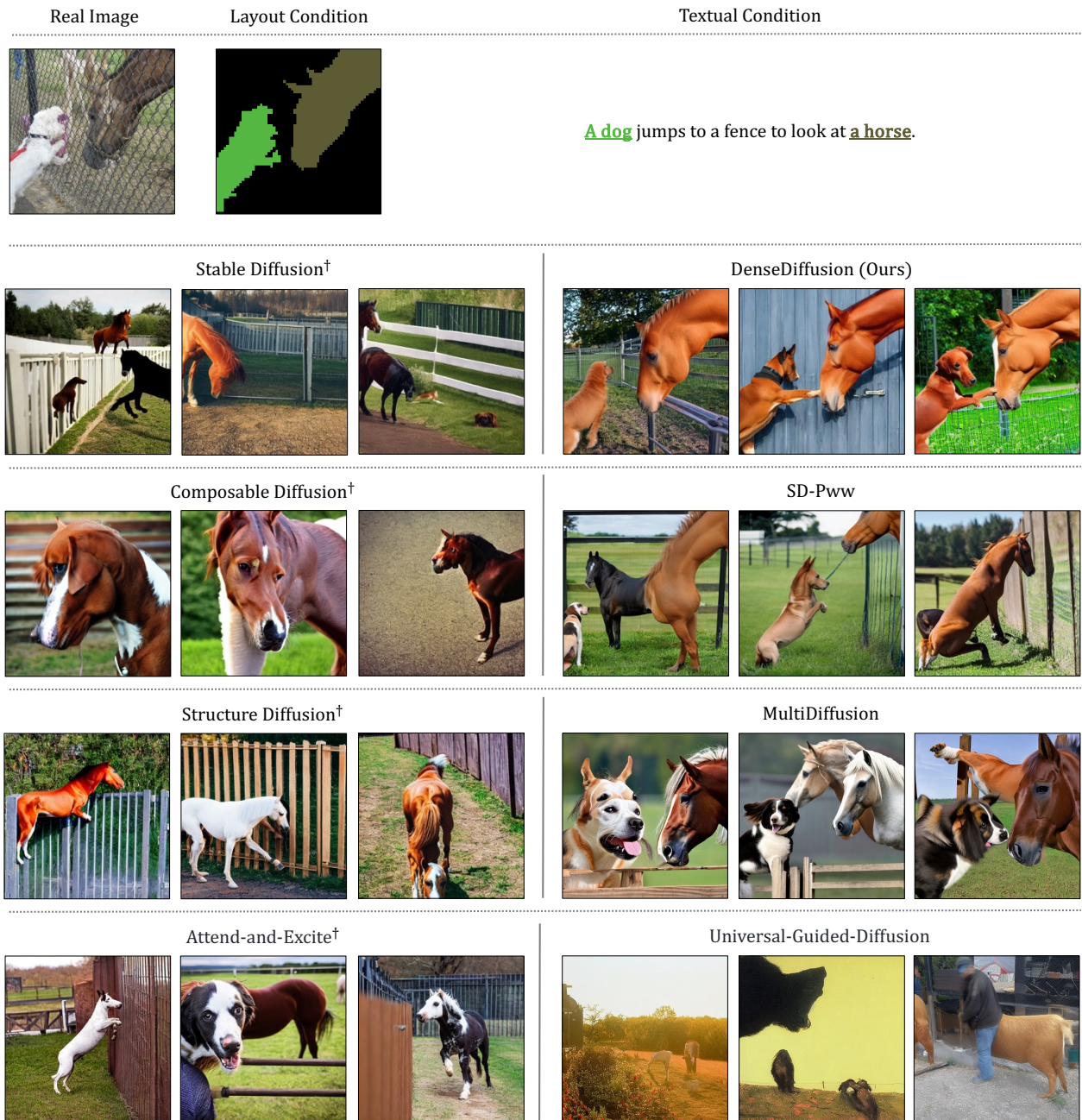


Figure 14: Qualitative comparison with additional methods. Methods denoted with [†] receive textual condition only.